Dental Traumatology

Dental Traumatology 2011; **27**: 356–367; doi: 10.1111/j.1600-9657.2011.01010.x

Development of new artificial models for splint rigidity evaluation

Christine Berthold[1], Friedrich Johannes Auer[2], Sergej Potapov[3], Anselm Petschelt[1]

[1]Dental Clinic 1 – Operative Dentistry and Periodontology, Friedrich-Alexander-University, Erlangen; [2]Dental Clinic Dr. Wiedenmann, Nuremberg; [3]Institute for Medical Informatics, Biometry and Epidemiology, Friedrich-Alexander-University, Erlangen, Germany

Correspondence to: Dr. Christine Berthold, Dental Clinic 1 – Operative Dentistry and Periodontology, Friedrich-Alexander-University Erlangen-Nuremberg, Glueckstr. 11, 91054 Erlangen, Germany
Tel.: +49 9131 85 34638
Fax: +49 9131 85 33603
e-mails: berthold@dent.uni-erlangen.de; christine_berthold@yahoo.de

Accepted 14 April, 2011

Abstract – *Aim:* We developed two versions of an artificial model and assessed their suitability for splint rigidity evaluation. These models allowed the simulation of traumatically loosened teeth and the use of the acid-etch technique for splint application. *Materials and methods:* A straight and half-round arch bar model with bovine tooth facets were manufactured. Using the Periotest method, tooth mobility was evaluated before (PTVpre) and after (PTVpost) splinting. Two types of previously investigated wire-composite splints, WCS1 (Dentaflex 0.45 mm; Dentaurum) and WCS2 (Strengthens 0.8 × 1.8 mm; Dentaurum), were applied ($n = 10$) to each model. The relative splint effect (SpErel = ΔPTV/PTVpre) was calculated, and the working times for the models and splints were evaluated. Student's *t*-test and the Mann–Whitney *U*-test were employed with Bonferroni correction for multiple hypotheses. *Results:* When comparing the relative splint effect of the 'injured' central incisors between the models within one splint type, differences were only found for tooth 21 (WCS2; $P < 0.008$); for comparisons of splints within one model type, differences were detected for both incisors and model types ($P < 0.008$). With the straight model, significantly less working time was necessary ($P < 0.05$). *Conclusion:* Using these models for *in vitro* splint rigidity evaluation, the splints can be applied with the acid-etch technique and tooth mobility can be individually adjusted. WCS1 is considered flexible compared to the more rigid WCS2. The results from the straight and the round model were predominantly closely related to each other. In terms of working time, the straight model is superior to the round model.

Splinting is one pillar in the treatment of dentoalveolar injuries involving traumata to the periodontal ligament (PDL) in the form of dislocation injuries and to the hard tissues such as alveolar bone and horizontal root fractures. Splinting secures the traumatized teeth or fragments in their original positions, preventing ingestion or inhalation and protecting the teeth and their surrounding tissues against traumatic forces during the vulnerable healing period. It is important that splints provide adequate rigidity dependent on the type of injury (1–3). For dislocation injuries, the splint should allow the transmission of physiological load to the teeth to improve healing (4, 5). To fulfill these requirements, wires (1, 2, 6), prefabricated metal (2, 7), or fiber-reinforced composite profiles (8, 9) are predominantly used in combination with the acid-etch technique. Factors influencing splint rigidity include the selection of the resin composite or reinforcing material (2, 9), the dimension of the adhesive points (10), and the splint position.

Various methods can be applied to evaluate splint rigidity. In addition to subjective methods that are too imprecise to discriminate between slight mobility changes (11), a broad variety of objective tooth and implant mobility evaluation techniques is available. These methods include static methods such as universal testing machines (12, 13), periodontometry (9, 14), and holographic interferometry (15, 16), as well as dynamic methods such as the Periotest method (1, 2, 6, 7, 17, 18) and resonance frequency analysis (19–21). Various studies in periodontology (22, 23), traumatology (1, 2, 6, 17, 24, 25), orthodontics (10, 26, 27), and implantology (21, 28) have been published concerning tooth and implant mobility evaluation with the Periotest device.

Studies focusing on splint rigidity evaluation were conducted *in vivo* on healthy (1, 7, 24, 25, 29) or injured humans (6, 24). For *in vitro* studies, artificial, individually created (10, 30), or commercially available and modified (2, 12, 13) phantom models or animal models (9) have been utilized. The advantages of splint rigidity testing with artificial models are the accessibility, ease of application and removal of the splints, and the wide variety of applicable tooth mobility-measuring techniques. However, for splint attachment, one disadvantage of artificial models consisting of plastic teeth is the lack of an etchable and bondable surface similar to the enamel in natural teeth.

The aim of this study was to develop two versions (straight and half-round arch bar models) of an artificial model for splint rigidity evaluation. These models were designed to allow simulation of traumatically loosened teeth as well as the use of the acid-etch technique for splint application. By testing the rigidity of two previously investigated wire-composite splints (WCS) (1, 2), the models were assessed for suitability and practicability for *in vitro* splint rigidity evaluation. We investigated the following null hypotheses: (i) the horizontal (h) Periotest values (PTVs) before splinting (pre) for the 'injured' teeth are not significantly higher than for the 'non-injured' teeth; (ii) there are no statistically significant differences in PTVpre between the two models; (iii) significant differences exist between the two models in terms of the relative splint effect (SpErel) per splint type; (iv) when comparing the two splint types per model type, no statistically significant differences occur in terms of SpErel; and (v) the working times for the two models are not significantly different from each other.

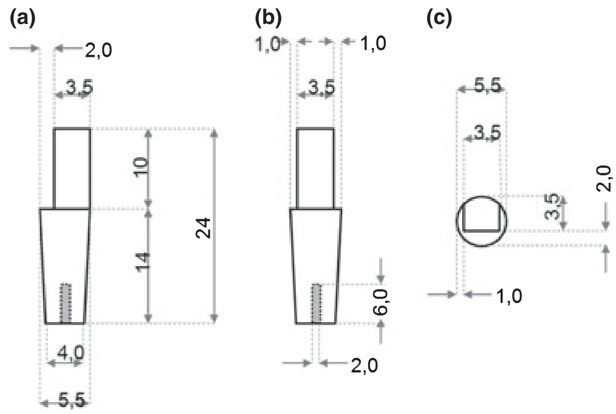

Fig. 1. Engineering drawing of a simulation tooth. All measurements are in mm. (a) Lateral view. (b) Front view. (c) Top view.

Materials and methods

Model manufacturing

A straight and a round model were developed and designed. The manufacturing was conducted in the workshop at the Dental Branch of the University of Erlangen.

Teeth

To produce the artificial teeth, a V2A stainless steel round profile (Ø 6 mm; REMAG AG, Nuremberg, Germany) was cut into 40-mm-long pieces. To simulate the tapered form of a root, the round profile was conically shaped with a lathe (Weiler, Emskirchen, Germany). For placement of the adjusting screw, a central hole was drilled at the apical end of the root, followed by cutting an internal thread (Ø 2 mm). Using a milling machine (FB1; Friedrich Deckel AG, München, Germany), three perpendicular plane surfaces (vestibular and proximal aspects) were shaped in the crown area for seating the bovine tooth facets. The surplus material of the round profile was sawn off, resulting in a simulation tooth with a total length of 24 mm (Fig. 1).

Rectangular tooth facets (3.5 × 10 mm) were sectioned from the middle of the crown of mandibular central permanent bovine teeth using a water-cooled low-speed saw (Isomet; Buehler, Duesseldorf, Germany). The facets were bonded to an object slide by their labial surfaces and then ground down with silicon carbide paper (120, 500 Grit, 200 rpm; Buehler) to a standardized thickness of 2 mm using a thin-section specimen holder (Buehler) and a grinding machine (Phoenix 4000; Buehler). The prepared tooth facets were stored in deionized water at 8°C until used.

To securely attach the tooth facets to the metal teeth, the coronal plane vestibular surface was silica coated (Rocatec Pre and Rocatec Plus; 3M ESPE, Neuss, Germany) and silanized (Silane; DMG, Hamburg, Germany). The plane-ground dentin site of the tooth facets was conditioned by the acid-etch technique using 37% phosphoric acid (Etching Gel; DMG), followed by application of a dual-cured dentin adhesive system (LuxaBond; DMG). The prepared facets were then attached to the vestibular coronal aspect of the metal teeth using a dual-cured resin composite luting material (LuxaCore Z; DMG). All materials were used as recommended by the manufacturer.

Jaw base and back panel – straight model

To manufacture the jaw base, the six aspects of a square aluminum profile (20 × 20 × 60 mm AlCuMgPb; Metallstore, Dornburg, Germany) were exactly plan-parallel shaped using the milling machine. The alveolar socket preparation procedure for teeth 13–23 is shown in Table 1; the central incisors served as the 'injured' teeth. Therefore, the alveolar sockets of the central incisors (teeth 11 and 21) were enlarged (Table 1, Fig. 2a) to allow increased tooth mobility compared to the basic preparation in the case of the lateral incisors (teeth 12 and 22) and the canines (teeth 13 and 23; Fig. 2b). To countersink the head of the apical adjusting screws (M2 × 8 mm; Lober & Schramm, Reutlingen, Germany), the 2-mm drill holes on the apical aspect of the jaw base were enlarged using a 4-mm spiral drill (Hoffman Group, Nuremberg, Germany). Three holes with an internal thread (M5 × 5 mm) were prepared (Fig. 3) to allow a screw joint between the back panel and the jaw base.

Table 1. Step-by-step preparation procedure for the alveolar sockets (teeth 13–23). Spiral drills 1–9 and the corresponding drilling depth were used for all sockets. For enlarging the sockets of the 'injured' teeth (11 and 21), step 10 was carried out

Drilling step	Ø spiral drill (mm)	Depth (mm)
1	2.0	20.0
2	5.0	13.0
3	5.2	11.0
4	5.5	8.00
5	5.7	6.00
6	5.8	4.00
7	6.0	3.00
8	6.2	1.00
9	Tapered reamer	15.0
Enlarging procedure for 'injured' teeth 11 and 21		
10	7.0	10.0

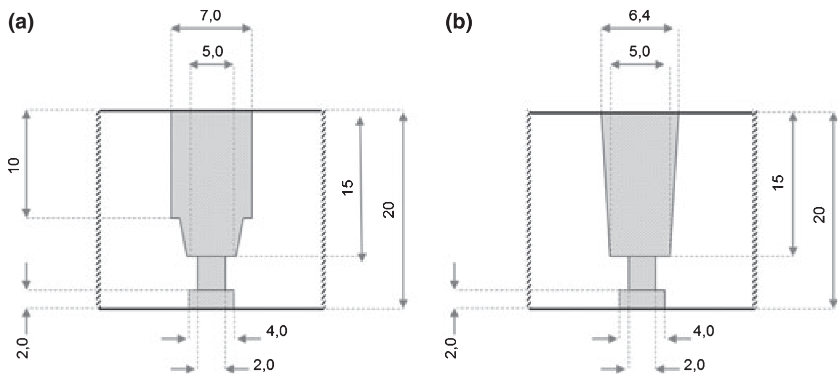

Fig. 2. Engineering drawing of the alveolar sockets. All measurements are in mm. (a) The enlarged sockets of 'injured' teeth 11 and 21. (b) The regular sockets of 'uninjured' teeth 13, 12, 22, and 23.

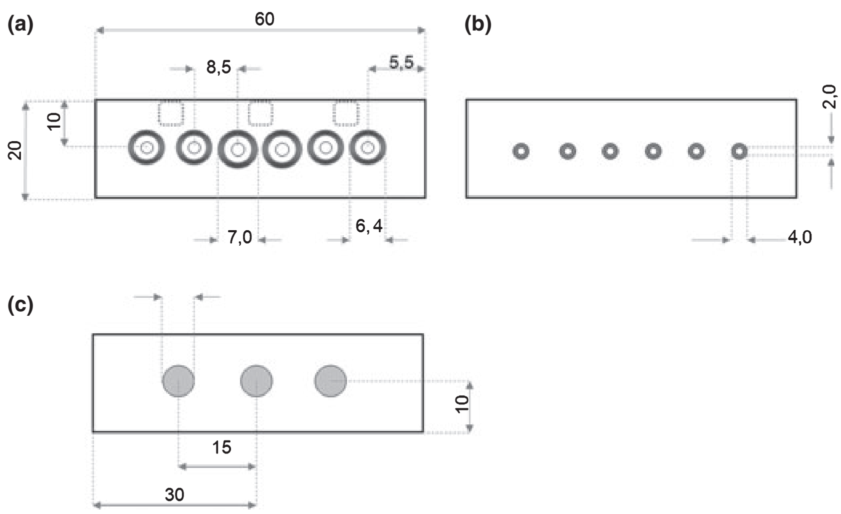

Fig. 3. Engineering drawing of the jaw base of the straight model. All measurements are in mm. (a) Top view. (b) Bottom view. (c) Back view.

For manufacturing the back panel, the six aspects of a rectangular aluminum profile (35 × 10 × 60 mm AlCuMgPb; Metallstore) were plan-parallel milled. Corresponding to the position of the screw holes at the back of the jaw base, three holes (Ø 5 mm) were drilled in the back panel and the holes were enlarged (3 mm deep) at the outer aspect using a countersink. To screw joint both components, countersunk screws (M5 × 13 mm; Lober & Schramm) were utilized.

Jaw base – round model

The top and bottom aspects of an aluminum round profile (Ø 60 × 20 mm AlCuMgPb; Alu-Verkauf, Hildesheim, Germany) were plan-parallel milled. The preparation of the alveolar sockets followed a similar procedure as described for the straight model (Figs 2 and 4). To allow precise positioning of the jaw base in the model holder during the measuring procedure, a central hole (Ø 5 mm) for the fixation screw (M5 × 60 mm) and six holes (Ø 2 mm) for the positioning screws (M2 × 30 mm) were drilled. From the coronal aspect, the six holes were enlarged (3.9 × 2 mm) to countersink the head of the positioning screws (Fig. 4).

Periodontal ligament

To create a standardized periodontal gap between the root and the alveolar socket, the roots were circumferentially wrapped with 0.4 mm of tin foil (0.1 and 0.3 mm tin foil; Dentaurum, Pforzheim, Germany). To ensure the vertical positioning of the teeth, metal washers (M2 0.3 × 5 mm; Norm Schrauben, Germering, Germany) were placed at the bottom of the alveolar socket. The prepared teeth were then placed into the sockets and the apical screws were adjusted. Using Impression Tray Resin LC (Henry Schein, Langen, Germany), a countermold was manufactured to fix the tooth position in the model. The coronal part of the teeth was attached to the mold with adhesive wax. The apical screws were then loosened and the countermold, including the teeth, was separated from the jaw base. The washers and the tin foil wrappings were removed. To produce the PDLs, the alveolar sockets were filled with low-viscosity impression silicon (Panasil Contact Plus; Kettenbach, Eschenburg, Germany) and then the countermold, including the teeth, was replaced. The apical screws were adjusted to ensure the central position of the teeth. After setting of the impression material, the screws and the countermold

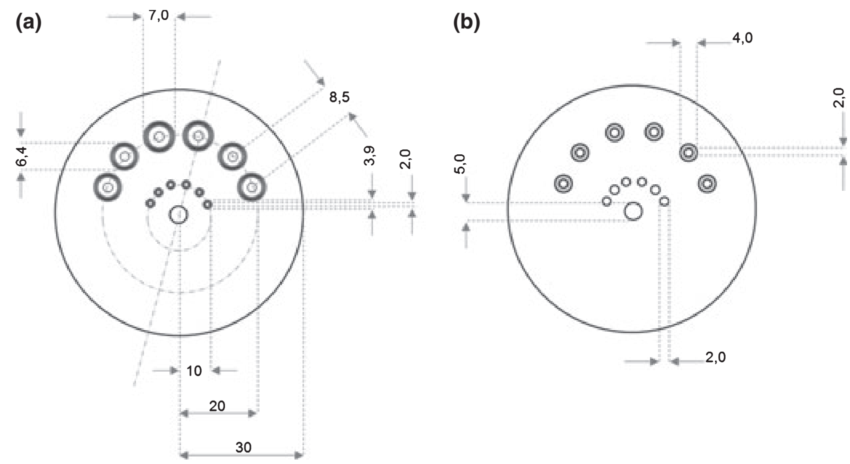

Fig. 4. Engineering drawing of the jaw base of the round model. The holes on the outer circle represent the alveolar sockets. The holes on the inner circle are for inserting the screws for positioning the model in the holder during the measuring procedure. All measurements indicated are in mm. (a) Top view. (b) Bottom view.

were removed and the excess silicon was trimmed with a scalpel. To allow a realistic simulation of increased mobility of the 'injured' central incisors, the silicon PDL was reduced by 10 mm from the coronal site and replaced with rubber foam (10 × 5 × 35 mm; Flexan, Waghaeusel, Germany; Fig. 5). The teeth were then repositioned into the corresponding alveolar sockets.

Model holder

A holder was manufactured for measuring tooth mobility in the round model. Two V2A stainless steel plates (30 × 150 × 150 mm; H & H Eisenmueller, Fellbach, Germany) were plan-parallel milled at all aspects. After drilling two corresponding holes and cutting internal threads through both metal pieces, the plates were perpendicularly screw joined together (Fig. 6). A hole was drilled (Ø 1.6 mm, 15 mm deep) in the back plate 21 mm from the edge, and an internal thread was cut for the positioning screw (M2 × 30 mm). A second hole (Ø 5 mm, 30 mm deep) 31 mm from the edge and aligned with the first hole was drilled for the central holding screw (M5 × 60 mm).

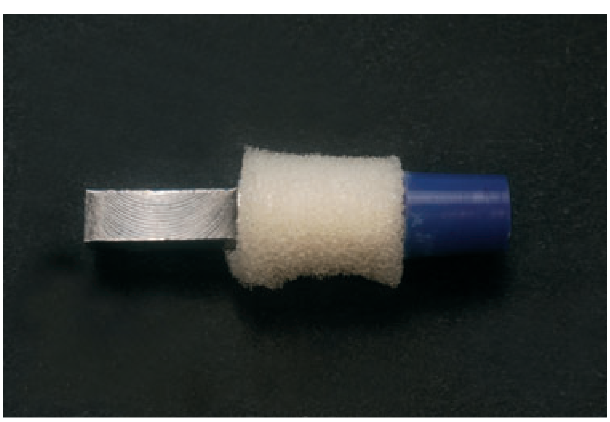

Fig. 5. 'Injured' tooth after partial replacement of the silicon periodontal ligament with rubber foam.

Model storage box

Individual storage boxes were prepared to allow wet storage of the natural tooth facets while simultaneously protecting the aluminum jaw base from water exposure. The tooth position of the models was transferred to the lids of two screw-cap polypropylene boxes (300 ml, Ø 90 × 57 mm; Pohli, Wuppertal, Germany), and then six holes were drilled for the teeth. Before placing the model on top of the box, a rubber dam with holes was placed over the teeth. The exposed coronal parts of the teeth were placed through the holes in distilled water, while the base remained dry outside the box.

Splint rigidity evaluation

The splint rigidity evaluation procedure is schematically shown in Fig. 7. Each splint type was applied 10 times. All tests were conducted by one investigator.

Tooth mobility adjustment

Tooth mobility was always set, before applying a new splint, on both models using the apical adjusting screws. Our aim was to achieve increased mobility for the

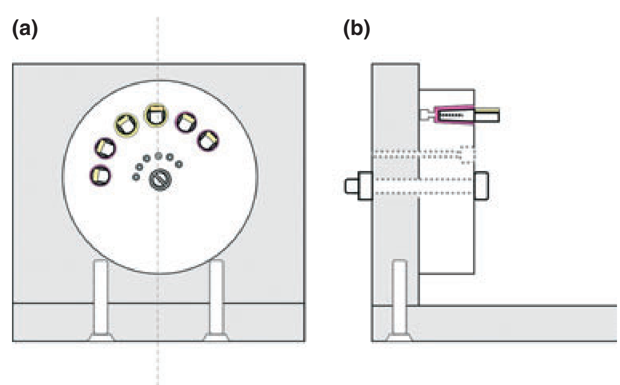

Fig. 6. Illustration of the model holder with the round model in position for measuring vertical tooth mobility.

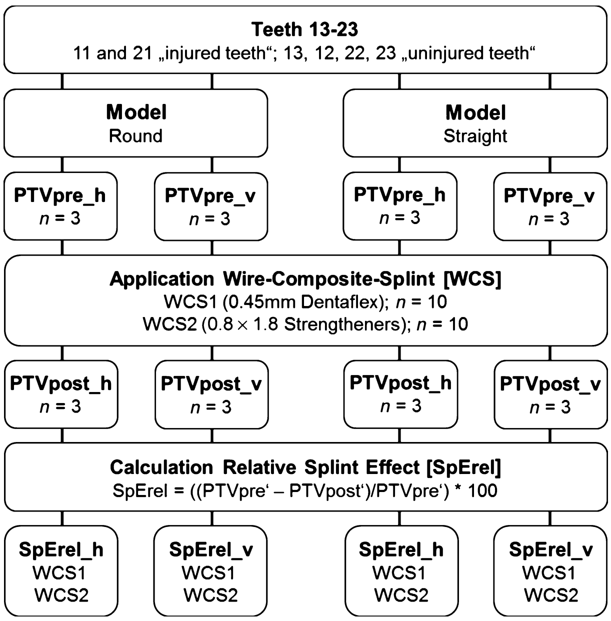

Fig. 7. Flow chart for splint rigidity evaluation of one passage. The Periotest values before splinting (PTVpre) were measured. After splint insertion, the Periotest values with the splint *in situ* (PTVpost) were evaluated and then the splint effect was calculated. WCS1, wire-composite splint 1 (0.45 mm Dentaflex); WCS2, wire-compoiste splint 2 (0.8×1.8 mm strengtheners); h, horizontal; v, vertical.

'injured' teeth and physiological mobility for the 'uninjured' teeth. The mobility during the adjusting procedure was monitored with the Periotest device (Gulden, Modautal, Germany) in the horizontal dimension. 'Injured' tooth 11 was set at degree-III loosening [horizontal PTVpre (PTVpre_h): $+35 \pm 2$], tooth 21 was set at degree-II loosening (PTVpre_h: $+25 \pm 2$), and 'uninjured' teeth 13, 12, 22, and 23 were set at a degree-0 loosening (PTVpre_h: range -1 to $+7$). Information regarding the correlation between the degree of loosening and the PTVs was obtained from the user guide of the Periotest device. The vertical PTVs before splinting (PTVpre_v) resulted from the adjusting process in the horizontal dimension.

Splinting

Two wire types with macroretentions were used to create WCS. A flexible orthodontic stainless steel wire (Dentaflex 0.45 mm, sixfold, straight wires; Dentaurum) was used and designated WCS1; a more rigid prosthodontic stainless steel wire (strengtheners 0.8×1.8 mm, coil; Dentaurum) was designated WCS2 (1, 2). For passively adjusting the two wire types to the half-round dental arch bar, different methods were used. The Dentaflex was first pulled over a mirror handle to achieve a near half-round shape. It was then customized to the arch bar with finger pressure. For curving the strengtheners, pliers were used and minor adaptations were made using finger pressure. In case of the straight model, the strengtheners were straightened with finger pressure. During the splint application procedure, the 'toot surface' was facing upwards to simulate a patient in a horizontal position. This was achieved by placing the round model in the holder and the flat model on the back panel. After conditioning the enamel surface with 37% phosphoric acid, the unfilled adhesive (Heliobond; Ivoclar Vivadent, Schaan, Liechtenstein) was applied and light cured. The previously adjusted wires were precisely attached to the middle of the tooth facets (sequence tooth 13, 23, 12, 11, 21, and 22) using light-curing flowable composite (Teric EvoFlow Bleach XL, Ivoclar Vivadent; Figs 8 and 9). The application of the splints alternated between WCS1 and WSC2 to reduce the influence of learning effect on the working time.

Tooth mobility evaluation

To assure reproducible measuring points, the middle of the tooth facet was marked. (1). The tip of the Periotest hand piece was aimed at these marked measuring points. Tooth mobility was measured every time before splint

Fig. 8. The straight model with the screw joint back panel. The bovine tooth facets were attached to the vestibular coronal aspect of the teeth. The simulation periodontal ligament for 'injured' teeth 11 and 21 (rubber foam) and for the 'non-injured' teeth (silicon) is *in situ*. Wire-composite splint 1 (0.45 mm Dentaflex) was attached with flowable composite to teeth 13–23 in the straight model.

Fig. 9. Wire-composite splint 2 (0.8×1.8 mm strengtheners) is depicted *in situ* on the round model.

application in the horizontal (PTVpre_h) and vertical (PTVpre_v) dimensions using the Periotest device. After splinting, tooth mobility was evaluated again in the horizontal (PTVpost_h) and vertical (PTVpost_v) dimensions with the splint *in situ*. All measurements were consecutively repeated three times per tooth (sequence 13, 12, 11, 21, 22, 22, and 23), and the mean horizontal and vertical PTVs were calculated out of the three measurements per tooth.

Splint removal
The splints were removed after tooth mobility evaluation. The composite points were reduced up to the wire without touching the tooth surface using a diamond bur (881KS; NTI, Kahla, Germany). After removing the wire, the remaining composite was gently reduced to a thin layer. The composite residuals were completely removed using a tungsten carbide bur (HM23R; Hager & Meisinger, Neuss, Germany).

Relative splint effect
Before calculating the splint effect relative to baseline (SpErel), the Periotest scale was adjusted from the original range of −8 to +50 to a scale with only positive values. Therefore, the measured PTVs were transformed (PTV' = PTV + 9). Using the transformed PTVpre' and PTVpost' measurements, calculation of SpErel in percent was performed:

$$\text{SpErel}\,[\%] = [(\text{PTVpre}' - \text{PTVpost}')/\text{PTVpre}'] * 100.$$

Working time
The working times, including the procedures of splint application, Periotest measurements, and splint removal, were documented for each splint. The total working time was calculated in seconds.

Statistical analysis

Descriptive statistics were performed for PTVpre, PTVpost, and SpErel, and the results were graphically displayed as box plots. The normal distribution was tested using the Kolmogorov–Smirnov test. For normally distributed data, Student's *t*-test was used; the non-parametric Mann–Whitney *U*-test was applied to non-normally distributed data. Probability values <0.05 were considered statistically significant.

The PTVpre of the 'injured' and 'non-injured' teeth were compared per model using the Student's *t*-test for unpaired samples. For multiple testing, the local significance level was adjusted using the Bonferroni correction ($\alpha' = \alpha/8 = 0.0063$). To test the PTVpre difference from 0 of the round and straight models, the Student's *t*-test with Bonferroni correction ($\alpha' = \alpha/6 = 0.008$) was applied. For comparing the SpErel values between the two models for each splint type, as well as comparing the two splint types for each model, the Mann–Whitney *U*-test with Bonferroni correction ($\alpha' = \alpha/6 = 0.008$) was used. The Student's *t*-test for unpaired samples was employed to compare the working times between the two models and between the two splints within one model type. Data were recorded using acquisition sheets and transferred to IBM SPSS STATISTICS 19.0 (IBM Corp., Somers, NY, USA). Statistical analysis was performed using the R Project for Statistical Computing (version 2.11.1; R Development Core Team 2010, http://www.r-project.org/).

Results

Mobility measurement

We recorded 2880 PTVs in total, 720 per splint and model. The three repeated PTVpre and PTVpost measurements per dimension and tooth were averaged; all calculations and statistical comparisons were based on this resulting mean.

Horizontal PTVpre (PTVpre_h)

The PTVpre_h of the 'injured' teeth ranged within the targeted limits, as described in Materials and methods. Tooth 11 underwent degree-III loosening (mean PTV 35.5 ± 1.5), while tooth 21 showed degree-II loosening (mean PTV 26.1 ± 1.2). The PTVpre_h for the 'non-injured' teeth ranged within the set limit of −1 to +7, a range equal to degree-0 loosening (Fig. 10).

The PTVpre_h of each 'injured' tooth (11 and 21) and each 'non-injured' tooth (13, 12, 22, and 23) were compared for each model type. Statistically significant differences were detected for all comparisons (Student's *t*-test/Bonferroni correction; $P < 0.0063$). For comparing the two models in terms of PTVpre_h, the difference was calculated using the following formula: $\Delta\text{PTVpre\_h}_{\text{Model}} = \text{PTVpre\_h}_{\text{Model round}} - \text{PTVpre\_h}_{\text{Model straight}}$. The difference from zero of $\Delta\text{PTVpre\_h}_{\text{Model}}$ for each tooth (Fig. 11) was tested using the Student's *t*-test and Bonferroni correction. Teeth 12, 11, 21, and 22 demonstrated no statistical significant differences ($P > 0.008$), while tooth 13 and 23 exhibited statistically significant differences ($P < 0.008$) in PTVpre_h between the two models.

Vertical PTVpre (PTVpre_v)

The mean PTVpre_v (Fig. 12) for the 'injured' teeth (tooth 11 = 3.8 ± 1.4; tooth 21 = 2.6 ± 1.0) were in general slightly higher than for the 'non-injured' teeth (tooth 13 = 1.2 ± 1.1; tooth 12 = 0.5 ± 1.5; tooth 22 = 1.7 ± 1.9; tooth 23 = −0.9 ± 1.3). The PTVpre_v values were compared between the models by calculating the difference using the following formula: $\Delta\text{PTVpre\_v}_{\text{Model}} = \text{PTVpre\_v}_{\text{Model round}} - \text{PTVpre\_v}_{\text{Model straight}}$. Statistically significant differences between the two models for ΔPTVpre_v were found for teeth 13, 12, 11, and 22 (Student's *t*-test/Bonferroni correction; $P < 0.008$; Fig. 11).

Horizontal PTVpost (PTVpost_h)

The mean PTVpost_h values of the 'injured' teeth were higher for WCS1 (tooth 11 = 30.4 ± 1.7; tooth 21 = 25.7 ± 2.0) than WCS2 (tooth 11 = 10.6 ± 1.3; tooth 21 = 11.0 ± 2.1). The same tendency was detected for the 'non-injured' teeth (Fig. 10).

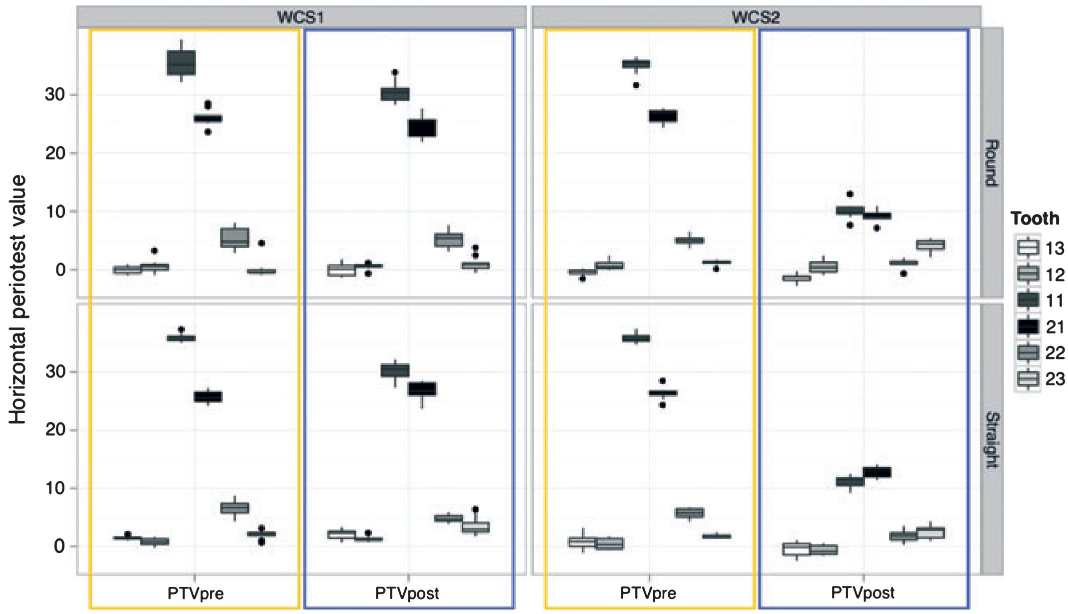

Fig. 10. Horizontal Periotest values before (PTVpre_h) and after (PTVpost_h) splinting, subdivided by the splint and model type for 'injured' teeth 11 and 21 and 'non-injured' teeth 13, 12, 22, and 23. The box (IQR, interquartile range) represents the 25th–75th percentile, the whiskers show the minimum and maximum, except for outliers (dots: 1.5–3 times of the IQR) and extreme values (asterisk: more than three times IQR).

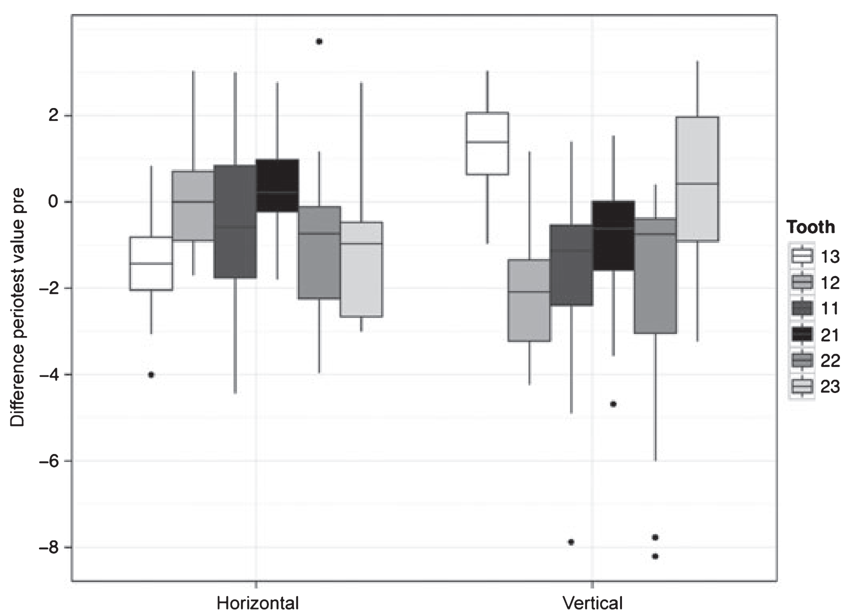

Fig. 11. Difference in the Periotest values before splinting (PTVpre) between the round and the straight models in the horizontal and vertical dimensions for 'injured' teeth 11 and 21 and 'non-injured' teeth 13, 12, 22, and 23. The box (IQR, interquartile range) represents the 25th–75th percentile, the whiskers show the minimum and maximum, except for outliers (dots: 1.5–3 times of the IQR) and extreme values (asterisk: more than three times IQR).

Vertical PTVpost (PTVpost_v)

The mean PTVpost_v measurements were, in general, higher in WCS1 than WCS2 for the 'injured' and 'non-injured' teeth (Fig. 12). This tendency was observed for both model types.

Horizontal SpErel (SpErel_h)

After adjusting the Periotest scale, SpErel was calculated in percent. The SpErel_h values for WCS1 and WCS2, subdivided for the round and straight models, are shown in Fig. 13. When comparing the SpErel_h of WCS1 and

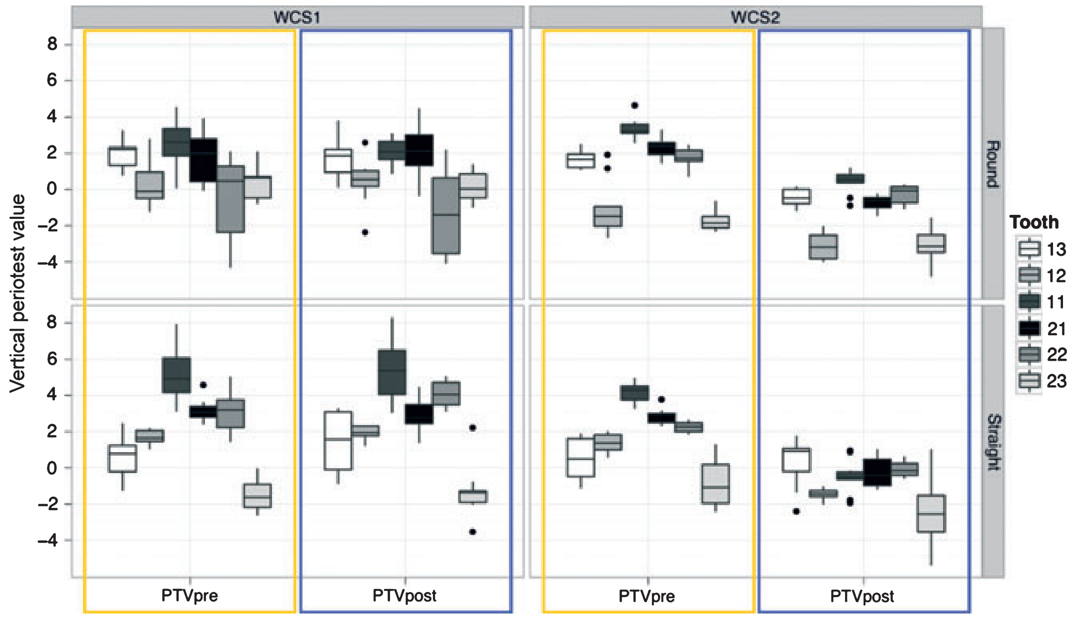

Fig. 12. Vertical Periotest values before (PTVpre_v) and after splinting (PTVpost_v) subdivided by the splint and model type for 'injured' teeth 11 and 21 and 'non-injured' teeth 13, 12, 22, and 23. The box (IQR, interquartile range) represents the 25th–75th percentile, the whiskers show the minimum and maximum, except for outliers (dots: 1.5–3 times of the IQR) and extreme values (asterisk: more than three times IQR).

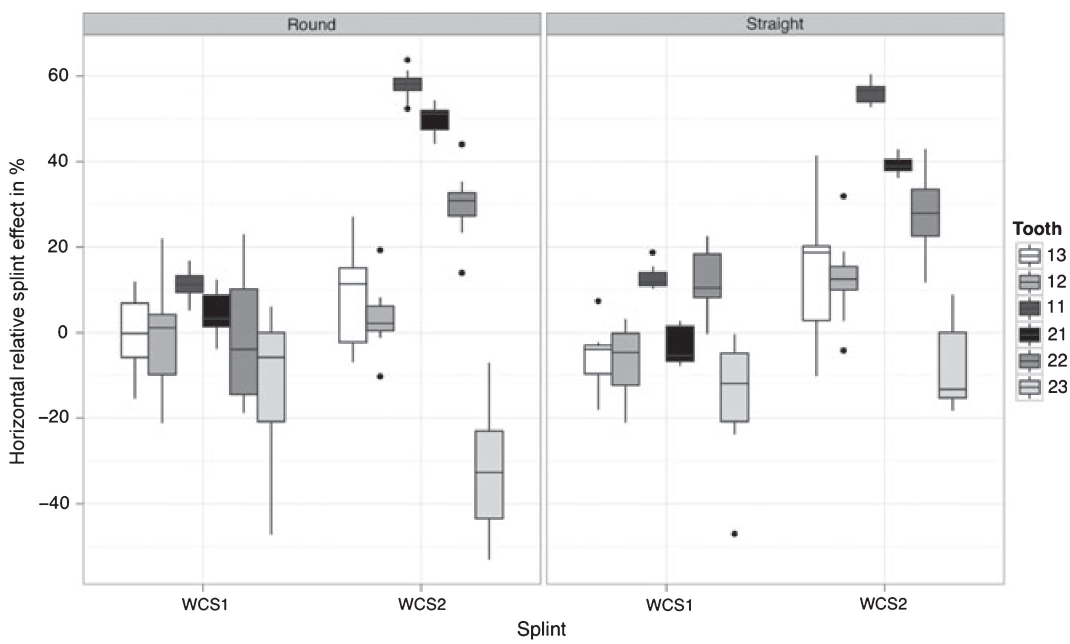

Fig. 13. Horizontal relative splint effect in percent subdivided by the splint and model types for 'injured' teeth 11 and 21 and 'non-injured' teeth 13, 12, 22, and 23. The box (IQR, interquartile range) represents the 25th–75th percentile, the whiskers show the minimum and maximum, except for outliers (dots: 1.5–3 times of the IQR) and extreme values (asterisk: more than three times IQR).

WCS2 within the straight model, statistically significant differences were found for teeth 13, 12, 11, 21, and 22 (Mann–Whitney *U*-test/Bonferroni correction; $P < 0.008$). Comparing the SpErel_h for the two splint types within the round model, statistically significant differences were detected for teeth 11, 21, and 22 (Mann–Whitney *U*-test/Bonferroni correction; $P < 0.008$).

The between-model comparisons of SpErel_h within one splint type revealed statistically significant differences for WCS1 in tooth 21 (Mann–Whitney *U*-test/Bonferroni correction; $P < 0.008$) and for WCS2 in teeth 21 and 23 (Mann–Whitney *U*-test/Bonferroni correction; $P < 0.008$).

Vertical SpErel (SpErel_v)

The SpErel_v calculations, subdivided by splint and model type, are illustrated in Fig. 14. Comparison of the

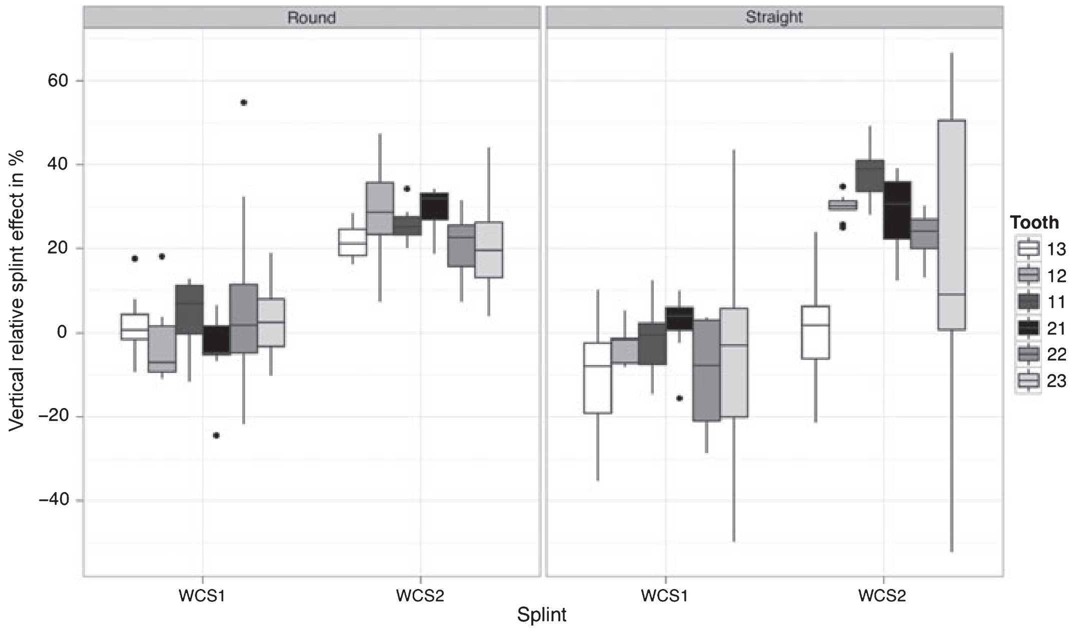

Fig. 14. Vertical relative splint effect in percent subdivided by the splint and model types for 'injured' teeth 11 and 21 and 'non-injured' teeth 13, 12, 22, and 23. The box (IQR, interquartile range) represents the 25th–75th percentile, the whiskers show the minimum and maximum, except for outliers (dots: 1.5–3 times of the IQR) and extreme values (asterisk: more than three times IQR).

SpErel values between WCS1 and WCS2 revealed significant differences within the round model for teeth 13, 12, 11, 21, and 23 (Mann–Whitney *U*-test/Bonferroni correction; $P < 0.008$), and within the straight model for teeth 12, 11, 21, and 22 (Mann–Whitney *U*-test/Bonferroni correction; $P < 0.008$).

No significant differences were detected for between-model comparisons of SpErel within a splint type.

Working time

The mean working time was calculated for each splint version per model and for each model independent of the splint type (Table 2). Statistically significant differences were detected when comparing the working times for the models (Student's *t*-test; $P < 0.05$). Less working time was necessary to conduct the experiments for the straight model. A within-model comparison of the working times for WCS1 and WCS2 revealed statistically significant differences for the round model (Student's *t*-test; $P < 0.05$) but not for the straight model (Student's *t*-test; $P > 0.05$).

Table 2. Working time (min) for the round and the straight model, independent from the splint as well as subdivided by splint type. Student's *t*-test ($\alpha = 0.05$) was carried out to compare the working time between the two models and the two splint types per model

Model	Round		Straight			
Splint	WCS1	WCS2	WCS1	WCS2	Round	Straight
Working time (s)						
Mean	39.1	39.7	31.4	31.6	39.4	31.5
SD	0.2	0.3	0.2	0.2	0.4	0.2
Min	38.9	39.3	31.2	31.3	38.9	31.2
Max	39.4	40.2	31.7	31.9	40.2	31.9
t-test	$P < 0.001$		$P = 0.100$		$P < 0.001$	

WCS1, wire-composite splint 1 (0.45 mm Dentaflex); WCS2, wire-compoiste splint 2 (0.8 × 1.8 mm strengtheners).

Discussion

Methodological factors

Various approaches have been used to evaluate the rigidity of splints (1, 2, 6, 7, 9, 12, 13, 30) or orthodontic retainers (10). *In vivo* tests on injured (6, 24) or non-injured humans (1, 7, 24, 25, 29) have different advantages, such as the presence of a natural PDL and of enamel for utilizing the acid-etch technique. The disadvantages, in the case of non-injured individuals, include the absence of increased tooth mobility (to simulate traumatized teeth) and the risk of unnecessary enamel damage during splint removal from perfectly sound teeth. When using injured individuals for splint rigidity evaluation, the teeth exhibit increased mobility; however, the data are usually widely spread, complicating data comparison. In addition, most of the tooth mobility measurement methods should not be applied to traumatized teeth, as additional damage may occur.

To benefit from the presence of natural PDL and enamel, dissected sheep mandibles were previously used for *in vitro* investigations (9). However, all front teeth exhibit highly increased mobility, and therefore the data are widely distributed. In addition, sheep mandibles are difficult to obtain, their shelf lives are limited, and they carry the potential risk of transferable infections such as Scrapie. Other studies were conducted on modified commercial (2, 12, 13) or individually prepared artificial models (10, 13). The manipulation of tooth mobility was achieved with adjusting screws (12, 13) or by removing or manipulating the anchoring mechanism (2) of the artificial teeth. Rubber dams or silicon were used to simulate the PDL (2, 12, 13). The advantages of artificial models include their unlimited storability, accessibility at any time, and the potential to adjust the tooth mobility to achieve similar initial values.

One major concern when using models consisting of plastic teeth is the lack of an etchable tooth surface for securely attaching the splints with composite (1, 2). Therefore, we aimed to design and develop a model that was durable, consisted of a near-natural simulation PDL, contained etchable enamel in the crown area, and was adjustable for tooth mobility. The planning for this model was based on the experience of using dissected sheep mandibles (31), modified commercial artificial models (2), and non-injured human volunteers (1). The aluminum jaw base was selected for its durability and, simultaneously, easy processing. V2A stainless steel was selected as the tooth material, as it exhibits superior longevity in comparison with plastic and possesses non-oxidation properties. The root was deliberately and abstractedly shaped in a conical form to allow easy and definite duplication. To simplify the manufacturing process of the teeth and the model base, the root dimension variation that occurs between natural incisors and canines (32) was abandoned. To provide an etchable enamel surface with properties similar to human enamel, permanent bovine central incisors were used to prepare the tooth facets (33, 34).

Before creating the simulation PDL, a pilot test was carried out to evaluate different gap widths between the root and the alveolar socket and different silicon materials. Our aim was to achieve model tooth mobility values for the 'non-injured' teeth similar to values obtained *in vivo* (1, 18, 25, 29). The sockets of the central incisors were enlarged as in cases of lateral dislocation injuries, simulating increased mobility. Interestingly, when the PDL gap was filled with silicon, it was not possible to obtain PTVpre_h values representative of degree-II or degree-III loosening. Increasing the gap width resulted in a decrease in the PTVpre_h measurements, an observation that can be explained by the elastic properties of silicon. As the thickness of the silicon layer increases, the accumulated energy of the deflecting force results in more rapid return of the tooth to its original position (35). Therefore, the silicon PDL of the 'injured' central incisors was partly removed (10 mm) from the coronal aspect and replaced with a layer of rubber foam, simulating a situation in the PDL gap after trauma that includes ruptured periodontal fibers and the presence of a hematoma at an early or organized stage. The rubber foam was selected after pilot tests with collagen fleece and gauze because of its superior durability and near-natural resetting properties, as in traumatized teeth.

The acid-etch technique is commonly used for attaching splints. To simulate the clinical situation, bovine tooth facets were attached to the coronal part of the model teeth to provide etchable enamel with properties similar to human teeth (33, 34). Although the width and height of the facets can vary, in this study the width of the facets was defined as 3.5 mm. Because we have extended the adhesive points over the mesiodistal distance, the width was set at 3.5 mm for all tests; therefore, the dimensions of the adhesive points did not vary. The influence of the adhesive point extension on the splint rigidity is currently under investigation.

Taking all these facts into consideration, the model is easy to handle, the attachment of the splints is similar to the clinical situation, and tooth mobility can be adjusted as required. The model was designed in two versions. The round version was intended to simulate the shape of the dental arch, and the straight version was designed to simplify splint application and reduce the working time. To prove whether this simplification is legitimate, the rigidity evaluations from different model types should be compared. To reduce the number of influencing and unknown factors, two previously investigated and well-established WCSs with different rigidity properties were utilized (1, 2, 31).

The Periotest device is a dynamic measuring method for objectively evaluating the damping characteristics of the PDL by quantifying the contact time of the tapping rod from the start until the end of the tooth deflection (18, 36). The advantages of this method include *in vitro* and *in vivo* applicability and easy handling. The Periotest method provides high reproducibility of the measurements when using defined reading points (1). In addition, the availability of previously published studies using the same tooth mobility evaluation method (1, 2, 6, 7, 17, 24–26, 29, 31) can be stated an advantage. Using this dynamic measuring method, the simulation PDL of the 'injured' central incisors needed to be brought closer to the clinical scenario after trauma. As found during the developing process of the models, thicker layers of silicon caused an accelerated resetting of the tooth after the deflection compared to thinner layers; therefore, the enlarged PDL gap of the 'injured' teeth was filled with rubber foam. We speculate that when applying static forces, as for example with a universal testing machine, only the thickness of the silicon layer itself and not the elastic properties of the 'simulated PDL' affect the mobility measurement outcome. The modification of the PDL of the 'injured' teeth by exchanging the silicon for rubber foam would thus perhaps not be necessary for static measuring methods. Further investigations will be carried out.

As a precondition for comparing the absolute splint effects, the PTVpre measured for the two WCSs and the two model types ought not to be significantly different. Because we were unable to fulfill this condition, the relative splint effect in percent (SpErel) was used for the comparison. Before calculating the SpErel, the PTV scale was corrected from the original scale (−8 to +50) to an adjusted scale (+1 to +59) to avoid division with PTVpre values near zero when calculating SpErel.

Study outcome

The horizontal and vertical PTVpre values of the 'injured' teeth were, for both models, significantly higher than for the 'non-injured' teeth (Figs 10 and 12). The increased mobility of the central incisors was required to simulate the situation in traumatically loosened teeth. To achieve this goal, the 'alveolar socket' of the two central incisors was enlarged compared to that of the lateral incisors and the canines, which served as 'non-injured' teeth. In addition, the simulated PDL for the central incisors was modified by partly replacing the silicon with rubber foam.

Comparing the PTVpre_h values of the two model versions, significant differences were found for teeth 13 and 23. For teeth 12, 11, 21, and 22, we were able to equalize the tooth mobility for both models (Fig. 11). It appeared to be easier to adjust the teeth with increased tooth mobility at an equal value, for both models, compared to the teeth presenting physiological tooth mobility. This observation may be explained by the thin layer of silicon used as the simulation PDL for the 'non-injured' teeth, resulting in a narrow adjustment range for tooth mobility. In addition, even when an equal preparation procedure is strictly emphasized for the alveolar sockets of both model versions, minimal variances can occur during manufacturing, leading to tooth mobility value differences. The PTVpre_v values were not actively manipulated, but rather resulted from the adjusting procedure of the PTVpre_h. Thus, statistically significant differences were detected for teeth 13, 12, 11, and 23 when comparing the PTVpre_v values for both model types (Fig. 11).

The between-model comparisons of SpErel within the splint types revealed few statistically significant differences, with the exception of the horizontal dimension of teeth 21 (WCS1), and 21 and 23 (WCS2) (Fig. 13). In the vertical dimension, significant differences for the two models within one splint type were found for teeth 13 and 11 (WCS2) (Fig. 14). The slight differences in SpErel may result from the different model geometries; however, as it is questionable whether similar results could be obtained by comparing two different models with the same design, further investigation is required. One between-model difference for SpErel emerges within the canines. These teeth are located at the end of the straight and the round dental bar, as the splints were always attached first to tooth 13, then to tooth 23, and then to teeth 12, 11, 21, and 22. Although the wires were adapted to the dental bar to fit passively, slight active forces within the wires or the polymerization stress of the flowable composite used for the splint attachment could cause differences in SpErel, especially for the canines (37).

Comparing SpErel for the 'injured' teeth of the two splint versions within one model type, statistically significant differences for each model in the horizontal dimension were found (Fig. 13). In most cases, the tooth mobility of the lateral incisors was also differently influenced by the two splint types. WCS2 produced higher splint effects compared to WCS1, causing a massive decrease in tooth mobility, especially in the horizontal dimension. Therefore, WCS2 is more rigid than WCS1, a result in agreement with previous *in vivo* (1) and *in vitro* studies (2, 31).

The working time for the round and the straight models varied greatly, independent of splint type (Table 2). The observed differences were mainly caused by the more complex adaptation process of the wires to the round model. In addition, the application of the wires to the straight dental bar appeared to be easier. When comparing the two splint types within the straight model, no statistically significant differences in working time were detected. The adaptation and the application procedure of the two different wires took an equal amount of time. The comparison of the working time for the two splint types within the round model revealed statistically significant differences; the working time for WCS2 was longer than for WCS1, which may be explained by the more complex adaptation procedure for WCS2.

Conclusion

Within the limits of *in vitro* testing, the developed models can be utilized for splint rigidity evaluation. Tooth mobility can be individually influenced and adjusted for 'injured' and 'non-injured' teeth by manipulating the socket size, PDL consistency, and the apical adjusting screws. Using bovine tooth facets, bonded to the coronal part of the simulation teeth, the splints can be securely attached with the acid-etch technique. The results of splint effect evaluation using the two introduced models are consistent with previous reports. WCS1 can be considered more flexible than WCS2.

The rigidity test results from the straight and the round models are predominantly related. The straight model was superior in terms of working time. Within the limitations of this study, the substitution of the round, near-naturally shaped model with the abstractedly shaped straight model can be recommended for evaluating splint rigidity. However, information as working time and ease of application cannot be achieved under the near-clinical conditions when using the straight model.

Acknowledgements

The invaluable help of Hans Loew of the dental workshop, University Erlangen, during the manufacturing procedure is highly acknowledged.

References

1. Berthold C, Holst S, Schmitt J, Goellner M, Petschelt A. An evaluation of the periotest method as a tool for monitoring tooth mobility in dental traumatology. Dent Traumatol 2010;26:120–8.
2. Berthold C, Thaler A, Petschelt A. Rigidity of commonly used dental trauma splints. Dent Traumatol 2009;25:248–55.
3. Oikarinen K. Tooth splinting: a review of the literature and consideration of the versatility of a wire-composite splint. Endod Dent Traumatol 1990;6:237–50.
4. Andersson L, Lindskog S, Blomlöf L, Hedström KG, Hammarström L. Effect of masticatory stimulation on dentoalveolar ankylosis after experimental tooth replantation. Endod Dent Traumatol 1985;1:13–6.
5. Oikarinen K. Functional fixation for traumatically luxated teeth. Endod Dent Traumatol 1987;3:224–8.
6. Ebeleseder KA, Glockner K, Pertl C, Städtler P. Splints made of wire and composite: an investigation of lateral tooth mobility in vivo. Endod Dent Traumatol 1995;11:288–93.

7. von Arx T, Filippi A, Lussi A. Comparison of a new dental trauma splint device (tts) with three commonly used splinting techniques. Dent Traumatol 2001;17:266–74.
8. Andreasen JO, Andreasen FM, Mejare I, Cvek M. Healing of 400 intra-alveolar root fractures. 2. Effect of treatment factors such as treatment delay, repositioning, splinting type and period and antibiotics. Dent Traumatol 2004;20:203–11.
9. Oikarinen K, Andreasen JO, Andreasen FM. Rigidity of various fixation methods used as dental splints. Endod Dent Traumatol 1992;8:113–9.
10. Schwarze J, Bourauel C, Drescher D. Frontzahnbeweglichkeit nach direkter Klebung von Lingualretainern. Fortschr Kieferorthop 1995;56:25–33.
11. Laster L, Laudenbach KW, Stoller NH. An evaluation of clinical tooth mobility measurements. J Periodontol 1975;46:603–7.
12. Oikarinen K. Comparison of the flexibility of various splinting methods for tooth fixation. Int J Oral Maxillofac Surg 1988;17:125–7.
13. Stellini E, Avesani S, Mazzoleni S, Favero L. Laboratory comparison of a titanium trauma splint with three conventional ones for the treatment of dental trauma. Eur J Paediatr Dent 2005;6:191–6.
14. Mühlemann HR. Periodontometry, a method for measuring tooth mobility. Oral Surg Oral Med Oral Pathol 1951;4:1220–33.
15. Wedendal PR, Bjelkhagen HI. Dental holographic interferometry in vivo utilizing a ruby laser system II. Clinical applications. Acta Odontol Scand 1974;32:345–56.
16. Wedendal PR, Bjelkhagen HI. Dental holographic interferometry in vivo utilizing a ruby laser system. I. Introduction and development of methods for precision measurements on the functional dynamics of human teeth and prosthodontic appliances. Acta Odontol Scand 1974;32:131–45.
17. Filippi A, Pohl Y, von Arx T. Treatment of replacement resorption by intentional replantation, resection of the ankylosed sites, and emdogain – results of a 6-year survey. Dent Traumatol 2006;22:307–11.
18. Lukas D, Schulte W. Periotest-a dynamic procedure for the diagnosis of the human periodontium. Clin Phys Physiol Meas 1990;11:65–75.
19. Lachmann S, Jäger B, Axmann D, Gomez-Roman G, Groten M, Weber H. Resonance frequency analysis and damping capacity assessment. Part I: An in vitro study on measurement reliability and a method of comparison in the determination of primary dental implant stability. Clin Oral Implants Res 2006;17:75–9.
20. Lachmann S, Laval JY, Jäger B, Axmann D, Gomez-Roman G, Groten M et al. Resonance frequency analysis and damping capacity assessment. Part 2: Peri-implant bone loss follow-up. An in vitro study with the periotest and osstell instruments. Clin Oral Implants Res 2006;17:80–4.
21. Nkenke E, Hahn M, Weinzierl K, Radespiel-Troger M, Neukam FW, Engelke K. Implant stability and histomorphometry: a correlation study in human cadavers using stepped cylinder implants. Clin Oral Implants Res 2003;14:601–9.
22. Feller L, Lemmer J. Tooth mobility after periodontal surgery. SADJ 2004;59:407.
23. Schulte W, d'Hoedt B, Lukas D, Maunz M, Steppeler M. Periotest for measuring periodontal characteristics – correlation with periodontal bone loss. J Periodontal Res 1992;27:184–90.
24. Andresen M, Mackie I, Worthington H. The periotest in traumatology. Part II. The periotest as a special test for assessing the periodontal status of teeth in children that have suffered trauma. Dent Traumatol 2003;19:218–20.
25. Andresen M, Mackie I, Worthington H. The periotest in traumatology. Part I. Does it have the properties necessary for use as a clinical device and can the measurements be interpreted? Dent Traumatol 2003;19:214–7.
26. Levander E, Malmgren O. Long-term follow-up of maxillary incisors with severe apical root resorption. Eur J Orthod 2000;22:85–92.
27. Tanaka E, Ueki K, Kikuzaki M, Yamada E, Takeuchi M, Dalla-Bona D et al. Longitudinal measurements of tooth mobility during orthodontic treatment using a periotest. Angle Orthod 2005;75:101–5.
28. Meredith N. A review of nondestructive test methods and their application to measure the stability and osseointegration of bone anchored endosseous implants. Crit Rev Biomed Eng 1998;26:275–91.
29. Mackie I, Ghrebi S, Worthington H. Measurement of tooth mobility in children using the periotest. Endod Dent Traumatol 1996;12:120–3.
30. Mazzoleni S, Meschia G, Cortesi R, Bressan E, Tomasi C, Ferro R et al. In vitro comparison of the flexibility of different splint systems used in dental traumatology. Dent Traumatol 2010;26:30–6.
31. Berthold C. Untersuchungen zur Schienungstherapie dentoalveolärer Verletzungen. Halle, Saale: Universitäts- und Landesbibliothek; 2002.
32. Lee B. The dimensions of the roots of the human permanent dentition as a guide to the selection of optimal orthodontic forces. Aust Orthod J 2010;26:1–9.
33. Nakamichi I, Iwaku M, Fusayama T. Bovine teeth as possible substitutes in the adhesion test. J Dent Res 1983;62:1076–81.
34. Oesterle LJ, Shellhart WC, Belanger GK. The use of bovine enamel in bonding studies. Am J Orthod Dentofacial Orthop 1998;114:514–9.
35. Stevanov M, Baruthio J, Eclancher B. Fabrication of elastomer arterial models with specified compliance. J Appl Physiol 2000;88:1291–4.
36. Schulte W. The new periotest method. Compend Contin Educ Dent 1988;(Suppl 12):S410–7.
37. Prevost J, Granjon Y. An in vitro study of the passivity of splints in dental trauma. J Dent 1998;26:39–45.